

**STOCHASTIC WAVE FIELD SOLUTION OF THE 2D ELASTIC WAVE  
EQUATION BASED ON THE RANDOM FOURIER-STIELTJES INCREMENTS**

By

Jorge O. Parra, Ph.D.  
Brian J. Zook, Ph.D.  
Southwest Research Institute  
6220 Culebra Road  
San Antonio, Texas 78238  
Phone (210) 522-3284; Fax (210) 684-4822  
email: [jparra@swri.org](mailto:jparra@swri.org)

**To be published in the *Journal of Applied Geophysics***

April 2001

## ABSTRACT

An analytical solution of the stochastic wave equation is presented to model 2D heterogeneous geological environments. In the formulation, a plane-harmonic seismic wave propagates in a medium having random elastic properties in the horizontal and vertical directions. The 2D random field representation is introduced in the stiffness properties of the medium by assuming it has log-normal probability density functions. The constitutive stress and displacement laws with the momentum balance equation for total stress yield a partial differential equation, which is developed using a perturbation approach by assuming a 2D random geological medium having material heterogeneity randomly distributed in the horizontal (x) and vertical (z) directions. The method yields a double integral representation of the displacement wave vector based on the Green's tensor and the Fourier-Stieltjes increments. The double integral is reduced to one integral representation by removing the singularities. The final form of the integral is used to construct the stochastic wave field displacement components expressed in terms of a single integral that is appropriate for calculations.

This paper also describes a numerical approach that predicts the stochastic wave field used to test the applicability of the theory by simulating a 2D randomly heterogeneous geological medium. Synthetic vertical and horizontal component seismograms based on this random medium indicate a decrease in wave amplitude and wave broadening effects at different depths of the random velocity images. The results suggest that the attenuation and dispersion of waves traveling between two wells are caused by the presence of scatterers observed in the 2D random velocity distribution. Large scatterers produce strong reflections that are observed in the random horizontal wave field seismograms. In general, the random wave field seismograms show characteristic seismic signatures that are associated with the structural distribution of the heterogeneities. In particular, random wave field signatures associated with heterogeneous low velocity zones are observed in the simulations. This kind of signature has been observed in crosswell data recorded at the Gypsy test site in Oklahoma.

## INTRODUCTION

Seismic signals propagating through heterogeneous materials experience a variety of effects, depending on the ratio of wavelength to scale of the heterogeneities. The major effort in seismic exploration is to analyze the interaction of seismic waves with geological interfaces and determine an appropriate model of the subsurface formations. Such model structures do not take into account small-scale heterogeneities as revealed by the logs and core samples. In particular, velocity and density fluctuations are at smaller scales, down to the microscopic pores and cracks known to exist within a geologic medium, and they cannot be resolved with current methods in a deterministic way. In addition, it has been shown that small-scale variations can have a significant effect on the transmitted wave field and can give rise to apparent attenuation and dispersion (O'Doherty and Anstey, 1971). The effect of scattering attenuation has been addressed by Brown and Seifert (1997). They demonstrated that the heterogeneous shale sandstone structure at the Gypsy test site, Oklahoma, produces an apparent horizontal velocity low at the crosswell seismic scale.

Synthetic seismic data produced using deterministic models cannot explain the significant variability observed in seismic field data. One alternative is a model that combines large- and

small-scale inhomogeneities. Large-scale inhomogeneities are the mean characteristics of the earth, while small-scale inhomogeneities are fluctuations in those mean values. The small-scale inhomogeneities are numerous and irregularly distributed, so the only information we can reconstruct from the seismic data are their statistical rock physical properties. To address this problem, several researchers have used solutions of the inhomogeneous elastic wave equation. There is extensive information in the applied physics literature on the solution of elastic wave propagation in heterogeneous media, and on statistical studies of various wave propagation phenomena and transport processes. The heterogeneous wave equations have been treated by a variety of methods based either on approximate multiple-scale expansions for periodic media (Santosa and Symes, 1991) or on various perturbation methods for statistical continua (Hoffman, 1964; Keller, 1964). Seismic wave propagation in random media in reference to dispersion and attenuation has been addressed by Korn (1993) and by Lerche and Petroy (1986), and seismology studies to describe small scale inhomogeneities have been addressed by several authors (Kerner, 1992; Ikelle et al., 1993; Kneib and Kerner, 1993; Roth and Korn, 1993). Some of these authors used the finite-difference algorithm to simulate seismic wave propagation. Only recently was a direct approach introduced to solve the 1D inhomogeneous wave equation in which the spatial velocity and density distributions are viewed as stochastic processes, and the effects on waves propagating through the random medium are described in terms of statistical averages of many observations. As addressed by Parra et al. (1999a) for the 1D stochastic solution, statistical parameters that define heterogeneities in terms of the rock physical properties of interest are the mean, variance, and fluctuation length scales.

In this paper, to produce synthetic seismograms in random media, the solution of plane-harmonic seismic waves in 1D random media having density and compressional wave velocity properties distributed in the vertical direction is extended to simulate a geologic medium having rock physical properties distributed in the horizontal ( $x$ ) and vertical ( $z$ ) directions. This work has several advantages. It obtains a solution expressed in terms of the standard statistical parameters of 2D random media, including the second-order moments (the variance and mean values of random physical material properties). In addition, the solution is an explicit integral representation of vector wave displacement based on the Green's function, and so by replacing the Green's function the theory may be readily extended to additional dimensions and alternate formations. The random wave field is expressed in terms of the coefficients of the Green's tensor, which are nonlinear functions of the elastic parameters. That is, after the expansion the solution remains a nonlinear function of the average rock properties of the medium and linear with respect to the standard deviations. An additional advantage of the present solution is to be able to simulate the two component seismic coda based on different degrees of variability of the material properties, angles of incidents, and average rock physical properties. The solution takes advantage of the small-scale heterogeneities determined from sonic logs to simulate seismic waveforms. For this purpose, a 2D random univariant Gaussian field with an exponential decay correlation function is introduced.

We expect that this modeling approach can be used to simulate small-scale heterogeneities to interpret seismic waveforms by analyzing the pulse broadening effect, the seismic coda, and the anisotropic behavior. This modeling can be done using well log and core information. Thus, such properties can be used to model 2D seismic data. Several stochastic replicas can be generated to explain observed data. Travel-time fluctuation, amplitude fluctuation, and attenuation and excitation of secondary waves can be analyzed. Since the solution is expressed

in terms of the  $\sigma$ -parameters (standard deviation of material property), medium variability is controlled by choosing these parameters to satisfy the first-order approximation.

To predict attenuation and velocity dispersion of seismic waves in randomly heterogeneous media, we suggest the work of Parra et al. (1999b), Shapiro et al. (1994), and Shapiro and Zien (1993). In Parra et al., a second-order perturbation solution of the ensemble-averaged 1D inhomogeneous wave equation provides the vector wave field and an effective wave propagation vector. These equations are expressed in terms of the standard deviations of the rock physical properties, the cross-correlation coefficient, and an integral that includes the spectral density function and a kernel function. The solution was compared with previously established theoretical work (e.g., Shapiro et al. 1994). This comparison resulted in a good correlation between both theories within the expected second-order accuracy. Although the 1D solutions given in Parra and Shapiro are based on different theoretical approaches, both arrive at the same results. However, the attenuation and velocity dispersion for 2D structures was not addressed by Shapiro. In addition, we used an elastic plane wave model (deterministic) to demonstrate the ability of stochastic medium theory to successfully address scattering on two length scales in real sedimentary lithology (Hackert and Parra 2000). The second-order perturbation solution of the displacement and wave propagation vector given in Parra et al. (1999b) can be extended to model 2D heterogeneities. These extensions are presently under consideration and will be reported in the near future. As for the 1D case (see Parra et al. 1999a), the present 2D stochastic wave field solution is the first step toward development of the second-order perturbation solution to the ensemble-averaged 2D inhomogeneous wave equation.

In summary, in this paper we extend the fundamental 1D random medium solution given in Parra et al. (1999a) to the 2D stochastic solution in the 2D space of the plane-harmonics of P- and S-wave propagation. Numerical models of the 2D solution are used to generate synthetic seismograms associated with a heterogeneous medium represented by a random medium. Random wave motion realizations are performed numerically using the method given by Shinozuka (1972).

## THEORY

The constitutive stress and the momentum balance equation are introduced in the development of the stress and displacement solutions for random increments using the 2D Fourier-Stieltjes increments representation. The first step is to establish the 2D inhomogeneous elastic wave equation based on the constitutive laws. The second step is to define the heterogeneous elastic properties as Gaussian random fields. In this application we assume the stiffness constants associated with the P- and S-wave velocities to be random fields. To facilitate the analysis we assume a linear approximation based on Taylor series to the first order in terms of  $\sigma$ -parameters for the vector wave displacement. The inhomogeneous Green's function is derived from the 2D elastic wave equation by applying this approximation. As a result of the derivation, source terms are obtained as random functions. The stochasticity arises from the spatially distributed form of the source. The source terms are functions of the stochastic random elastic properties.

To develop a tractable solution for random wave displacements, the 2D Fourier-Stieltjes integral is introduced and applied to the Green's function in the frequency domain. This requires expressing the source increments in terms of the normalized random fields of the stiffness constants using a theorem given in Parra et al. (1999a). The next step is to reduce the double

integral representation of the vector wave displacement to a single integral representation by removing the singularities. The final solution is further modified by introducing a numerical approach to evaluate the stochastic wave fields.

### General representation of the classical elastic wave equation/random coefficients

We have generalized the theory of elastic waves in unbounded media to allow the intrinsic properties to be heterogeneous, e.g., a randomly distributed spatial structure. To do this, we must extend the constitutive relations to a case of spatially variable coefficients. In the frequency domain these basic equations are:

$$\begin{aligned} \text{C} \quad & \text{Constitutive Stress/Displacement Laws:} \\ & \text{Total stress of the elastic medium} \\ & \tau_{ij} = 2\mu(\vec{x})e_{ij} + \lambda(\vec{x})\delta_{ij}e_{\alpha\alpha} \end{aligned} \quad (1a)$$

$$\begin{aligned} \text{C} \quad & \text{Momentum Balance Equation for Total Stress} \\ & \frac{\partial \tau_{ij}}{\partial x_j} = \nabla \cdot \tau = -\omega^2 [\rho(\vec{x})]u_i(\vec{x}) \end{aligned} \quad (1b)$$

where  $e(\vec{x}) =$  total volumetric strain, and  
 $u(\vec{x}) =$  displacement.

From the constitutive Equations (1a) and (1b) we obtain the differential equations in the frequency domain:

$$\frac{\partial}{\partial x_j} \left\{ \mu(\vec{x}) \left( \frac{\partial u_i}{\partial x_j} + \frac{\partial u_j}{\partial x_i} \right) \right\} + \frac{\partial}{\partial x_i} \left( \lambda(\vec{x}) \frac{\partial u_j}{\partial x_j} \right) + \omega^2 \rho(\vec{x})u_i = 0. \quad (2)$$

The elastic wave equation model problem in Equation (2) can be reduced to the solution of a plane wave propagating in the x and z planes of a 2D random geological medium having material heterogeneity randomly distributed in the horizontal (x) and vertical (z) directions. For this system of equations the following material properties (or random field coefficients) are considered:

$$\alpha(x,z) = \lambda(x,z) + 2\mu(x,z) = e^{A(x,z)} \quad (3a)$$

and 
$$\mu(x,z) = e^{B(x,z)}, \quad (3b)$$

where  $A(x,z)$ , and  $B(x,z)$  are assumed to be Gaussian random fields. The means of the log-coefficients are the geometric means of the coefficients themselves [see Parra et al. (1999a)]. Thus,

$$\begin{aligned} A(x,z) & \sim \text{Rn}(\alpha(x,z)) \sim \bar{A} \pm \sigma_A \text{AN}(x,z) \\ B(x,z) & \sim \text{Rn}(\mu(x,z)) \sim \bar{B} \pm \sigma_B \text{BN}(x,z), \end{aligned} \quad (4)$$

where 
$$\bar{A} \sim \text{Rn}(\alpha_G) : \alpha_G \sim e^{\bar{A}} \quad (5)$$

and  $\bar{B} \text{ ' Rn}(\mu_G) : \mu_G \text{ ' } e^{\bar{B}}$ .

Equations (3) suggest that we have defined AN and BN in such a way that they are normalized Gaussian random fields, with zero means and unit variances (the actual variances of A and B are  $\sigma_A^2$ , and  $\sigma_B^2$ ). We can rewrite the governing linear system of Equations (1) in terms of log coefficients given by

$$\alpha(x,z) \text{ ' } \alpha_G \exp(\sigma_A AN(x,z)), \quad (6)$$

and  $\mu(x,z) \text{ ' } \mu_G \exp(\sigma_B BN(x,z))$ .

Thus, the perturbation equations can be obtained by substituting Equations (6) into the governing linear system of equations, and by expanding the resulting elastic differential equation (EDE) in terms of  $\sigma$ -parameters:

and  $\sigma_A =$  standard deviation of Rn ( $\alpha(x, z)$ )  
 $\sigma_B =$  standard deviation of Rn ( $\mu(x, z)$ ).

Since there is more than one parameter, a multi-parameter expansion is required. That is, we expand the vector wave field to first-order in terms of the  $\sigma$  - parameters, thus neglecting terms of order  $O(\sigma^2)$  or higher, and then solve the resulting stochastic wave equation.

The solution of  $u_x(x, z, \omega)$  and  $u_z(x, z, \omega)$  must depend on the material property parameters  $\sigma_A$  and  $\sigma_B$ . We chose to determine the perturbation equations by applying Taylor series to  $u_x = u_x(x, z, \omega; \sigma_A, \sigma_B)$  and  $u_z = u_z(x, z, \omega, \sigma_A, \sigma_B)$  around the parameter values  $\sigma_A = \sigma_B = 0$ . Dropping the  $(x, z, \omega)$  dependence from our notations, we have

$$u_x(\sigma_A, \sigma_B) \text{ ' } u_{ox} \% u_A^{(x)} \sigma_A \% u_B^{(x)} \sigma_B \quad (7a)$$

and  $u_z(\sigma_A, \sigma_B) \text{ ' } u_{oz} \% u_A^{(z)} \sigma_A \% u_B^{(z)} \sigma_B \quad (7b)$

and  $u_x(0, 0) \text{ ' } u_{ox} \quad (8)$

$$u_z(0, 0) \text{ ' } u_{oz}.$$

Equations (7) specifically indicate that the total vector wave field can be obtained by a single superposition of  $u_x(0,0)$ ,  $u_z(0,0)$ ,  $u_x(\sigma_A, 0)$ ,  $u_z(0, \sigma_B)$ , etc.

The obvious meaning of these elementary wave fields is, for example:

$$A \text{ ' } \bar{A}, \text{ and } B \text{ ' } \bar{B}, \text{ or equivalently} \quad (9)$$

and  $\alpha \text{ ' } \bar{A}_G, \mu \text{ ' } \bar{\mu}_G$ .

For example,  $u_z(\sigma_B, 0)$  is the stochastic wave field for random  $B(x, z)$  and constants  $A(y,z)$ .

We will now develop separate equations for each of the sub-problem solutions defined in Equations (7) and (8).

### Representation of random source terms

The present approach consists of forming random vector functions for each material property. These functions are defined by the superposition of the deterministic and the random solutions, assuming linear approximations for the material properties.

Thus, the deterministic solution for the displacement is given by

$$\begin{aligned} u_x(0,0) &= u_{ox} \\ \text{and} \quad u_z(0,0) &= u_{oz}. \end{aligned} \quad (10)$$

The solution corresponds to  $\sigma_A = \sigma_B = 0$ .

For a plane wave traveling at an angle of incidence  $\theta$  with respect to the z-axis, the displacement components derived from potentials are given by

$$\begin{aligned} u_{ox} &= \delta_j k_{ox} e^{\delta_j (k_{ox} x_0 + k_{oz} z_0)} \\ \text{and} \quad u_{oz} &= \delta_j k_{oz} e^{\delta_j (k_{ox} x_0 + k_{oz} z_0)}, \end{aligned} \quad (11)$$

where  $(x_0, z_0)$  is the source position coordinate

$$\text{and} \quad k_{ox} = \frac{\omega}{v_p} \sin\theta, \quad k_{oz} = \frac{\omega}{v_p} \cos\theta, \quad (12)$$

$v_p$  is the compressional wave velocity of the medium.

Thus, the random vector displacement for the material property  $A(x,z)$  is given by:

$$\begin{aligned} u_z(\sigma_A, 0) &= u_{oz} + \sigma_A u_A^{(z)} \\ \text{and} \quad u_x(\sigma_A, 0) &= u_{ox} + \sigma_A u_A^{(x)}. \end{aligned} \quad (13)$$

Inserting these equations for  $\sigma_B = 0$  into Equation (2), and expanding the exponential  $\exp(\sigma_A A(x, z))$  using Taylor series,  $\exp(\sigma_A A(x, z)) = 1 + \sigma_A A(x, z)$ , and recognizing that the deterministic part of the linear system of equations vanishes, gives the first-order approximate equation in the frequency domain:

$$\langle u_A = F_A, \quad (14)$$

with the following vector notation:

$$u_A = [u_A^{(x)}, u_A^{(z)}]^T, \text{ and} \quad (14a)$$

$$F_A = [f_A^{(x)}, f_A^{(z)}]^T. \quad (14b)$$

$\nabla_{ij}$  is the differential operator of components  $\nabla_{ij}$ , given by

$$\nabla_{ij} = \begin{pmatrix} \alpha_G \frac{\omega}{V} + \mu_G \frac{\omega}{V^2} + \omega^2 \rho_G & (\lambda_G + \mu_G) \frac{\omega}{V^2} \\ (\lambda_G + \mu_G) \frac{\omega}{V^2} & \alpha_G \frac{\omega}{V} + \mu_G \frac{\omega}{V^2} + \omega^2 \rho_G \end{pmatrix}. \quad (15)$$

This system of equations is a stochastic wave equation for the displacement components  $u_A^{(x)}(x, z, \omega)$  and  $u_A^{(z)}(x, z, \omega)$ . This stochasticity arises only from the spatially distributed random source terms given by

$$f_A^{(x)} = \alpha_G \frac{\omega}{V} \left\{ AN(x, z) \left( \frac{M_{ox}}{V} + \frac{M_{oz}}{V} \right) \right\} \quad (16)$$

and

$$f_A^{(z)} = \alpha_G \frac{\omega}{V} \left\{ AN(x, z) \left( \frac{M_{ox}}{V} + \frac{M_{oz}}{V} \right) \right\}.$$

For the second material property  $B(x, z)$  the random vector wave displacement is given by:

$$u_z(0, \sigma_B) = u_{oz} + \sigma_B u_B^{(z)} \quad (17)$$

and

$$u_x(0, \sigma_B) = u_{ox} + \sigma_B u_B^{(x)}.$$

Substituting this equation in Equation (2) for  $\sigma_A = 0$ , and expanding the exponential (i.e.,  $\exp(\sigma_B BN(x, z)) = 1 + \sigma_B BN(x, z)$ ) using Taylor series, the first-order approximate equation in the frequency domain is reduced to

$$\nabla u_B = F_B, \quad (18)$$

$$u_B = \begin{bmatrix} u_B^{(x)} \\ u_B^{(z)} \end{bmatrix}^T, \quad (18a)$$

where

$$F_B = \begin{bmatrix} f_B^x \\ f_B^z \end{bmatrix}^T, \quad (18b)$$

in which

$$f_B^{(x)} = \alpha_G \frac{\omega}{V} \left[ BN(x, z) \left( \frac{M_{ox}}{V} + \frac{M_{oz}}{V} \right) \right], \quad (18c)$$

and

$$f_B^{(z)} = \alpha_G \frac{\omega}{V} \left[ BN(x, z) \left( \frac{M_{ox}}{V} + \frac{M_{oz}}{V} \right) \right]. \quad (18d)$$

The differential operator is given by Equation (15). In this case,  $BN(x, z)$  is a parameter associated with the shear wave velocity of the medium.

### First-order stochastic vector wave field

To find a solution of the first-order stochastic vector wave field based on Equation (7), we must determine the values of  $u_A$  and  $u_B$  vectors by inverting Equations (14) and (18). However, to solve these equations having nonlinear source terms, we use the 2D random Fourier-Stieltjes representation given by

$$f(x, z) = \int_{\mathbb{R}^2} \int_{\mathbb{R}^2} e^{j(k_z z + k_x x)} d\hat{f}(k_x, k_z, \omega), \quad (19)$$

for a random medium having material properties in the  $x$  and  $z$  directions (see Parra et al., 1999a).

After applying this representation to Equations (14) and (18), the spectral random increments of the displacements  $u_A$  and  $u_B$  are expressed in terms of the coefficients of the Green's tensor. These coefficients are determined together with the source increments in Appendix A. The increments allow us to write a general expression for the random vector wave field components as follows

$$\begin{pmatrix} d\hat{u}_x \\ d\hat{u}_z \end{pmatrix} = \begin{pmatrix} g_{11} & g_{12} \\ g_{21} & g_{22} \end{pmatrix} \begin{pmatrix} d\hat{f}_A & d\hat{f}_B \\ d\hat{f}_A & d\hat{f}_B \end{pmatrix} \begin{pmatrix} \sigma_A \\ \sigma_B \end{pmatrix}, \quad (20)$$

where the coefficients  $g_{ij}$  are nonlinear functions and the increments  $d\hat{f}$  are the source terms. These source terms are associated with the random material properties of the medium.

To find a tractable representation for the random vector wave field given in Equation (20), Appendix B gives a single integral representation for the components. That is, the double integral introduced by Equation (19) is reduced to single integrals by removing the singularities given implicitly in the coefficients of the Green's tensor (see Appendix C). The single integrals are incorporated into the random wave field components to yield a practical representation for calculations (see Appendix B). These random vector displacement components are given by

$$\begin{aligned} u_x(x, z, \omega) = & \pi j \sigma_A k_p^2 \int_{\mathbb{R}^2} G_1(t) d\hat{A}(x_p(t), z_p(t)) \\ & + \pi j \sigma_B k_p^2 \sin 2\theta \left[ \left( \frac{v_s}{v_p} \right)^2 \int_{\mathbb{R}^2} G_2(t) d\hat{B}(x_s(t), z_s(t)) \right. \\ & \left. + \int_{\mathbb{R}^2} G_3(t) d\hat{B}(x_p(t), z_p(t)) \right] \end{aligned} \quad (21)$$

$$\begin{aligned}
u_z(x, z, \omega) = & \pi j \sigma_A k_p^2 \int_{\hat{A}} G_1(\hat{t}) d\hat{A}(x_p(\hat{t}), z_p(\hat{t})) \\
& + \pi j \sigma_B k_p^2 \sin 2\theta \left( \frac{v_s}{v_p} \right)^2 \int_{\hat{B}} \left[ G_2(\hat{t}) d\hat{B}(x_s(\hat{t}), z_s(\hat{t})) \right. \\
& \left. + G_3(\hat{t}) d\hat{B}(x_p(\hat{t}), z_p(\hat{t})) \right]
\end{aligned}$$

( 2 2 )

where

$$\begin{aligned}
x_p(t) &= k_p [(1/a) \sin \theta + t \cos \theta] \\
z_p(t) &= k_p [(1/a) \cos \theta + t \sin \theta] \\
x_s(t) &= k_p \left[ \left( \frac{v_p}{v_s} \right) \sin \theta + t \cos \theta \right] \\
z_s(t) &= k_p \left[ \left( \frac{v_p}{v_s} \right) \cos \theta + t \sin \theta \right].
\end{aligned}$$

The final first-order solution in Equations (21) and (22) are linear with respect to the standard deviations of the random material properties A and B, and they are nonlinear with respect to the elastic properties of the medium. In addition, the kernels  $G_1$ ,  $G_2$  and  $G_3$  given in Appendix B are nonlinear functions, which have structures similar to those of a point source in an unbounded medium (see Aki and Richards, 1980). For example, the first term of Equation (21) is multiplied by  $\sigma_A$  and represents the compressional wave energy of the random wave field, and the second term is multiplied by  $\sigma_B$  and represents the shear wave energy of the random wave field. These two standard deviations control how much P- or S-wave energy should be considered for simulating random wave fields. In addition, the shear wave contribution term is multiplied by the factor  $\sin(2\theta)$ , which includes the angle of incidence of the plane wave. That is, for incidence angles of 0 and 90 degrees, the contribution of the shear wave energy is zero. Alternatively, for an angle of incidence equal to 45 degrees, the shear wave energy contribution to the total random wave field is maximum.

To generate wave field responses with the above integral solution we express the Fourier increments  $d\hat{A}$  and  $d\hat{B}$  in terms of the spectral density function (S) following the method of Shinozuka (1972). The numerical implementation for solution of the stochastic wave equation to generate wave fields is given in the next section.

## NUMERICAL APPROACH TO EVALUATE STOCHASTIC WAVE FIELDS

To simulate elastic property distribution associated with P- and S-wave velocities and wave field responses, we have implemented an algorithm based on the work of Shinozuka (1972). First we introduced expressions to calculate 2D distributions of random elastic properties, then we describe the numerical method to simulate the wave field. Finally, we give expressions for the density functions to calculate random elastic properties and address the wave field expressions associated with 2D elastic property distributions.

### Elastic properties

We consider the two elastic properties as random variables,  $\alpha=\lambda+2\mu$ , which are associated with the P- waves, and the rigidity  $\mu$ , which is associated with the S-waves. We assume that these random variables have a log-normal distribution — the natural logarithms of these quantities fit a normal distribution. Accordingly, we have defined two auxiliary quantities  $A$  and  $B$ :

$$\begin{aligned} A(x,z) & \tilde{N} \ln[\alpha(x,z)] + \bar{A}\sigma_A A\tilde{N}(x,z) \\ B(x,z) & \tilde{N} \ln[\mu(x,z)] + \bar{B}\sigma_B B\tilde{N}(x,z) \end{aligned} \quad (23)$$

In Equation (23) the symbols with bars indicate mean values, and the primed symbols are the random variables themselves with a mean of zero and a variance of one.

The integrals associated with the stochastic processes are all calculated using Fourier-Stieltjes representations:

$$\begin{aligned}
A(x,z) &= \int_{-\infty}^{\infty} \int_{-\infty}^{\infty} e^{jk_x x + jk_z z} d\hat{A}(k_x, k_z) \\
B(x,z) &= \int_{-\infty}^{\infty} \int_{-\infty}^{\infty} e^{jk_x x + jk_z z} d\hat{B}(k_x, k_z) .
\end{aligned} \tag{24}$$

After a change of variables using the relations given by Equations (C-2) and (C-10) in Appendix C, the double integration in Equation (24) is reduced to a single integral. In addition, the rms amplitudes of the random Fourier increments  $d\hat{A}(t)$  and  $d\hat{B}(t)$  are related directly to the spectral density function random field [see Shinozuka (1972, 1987) and Parra et al. (1999a)] , which is equal to the inverse Fourier transform of the covariance function (Wiener-Khinchine and Leperra - see Reif, 1965). Denoting  $S(x(t), z(t))$  as the spectral density function, we have the Fourier increments given by

$$\begin{aligned}
d\hat{A}(x(t), z(t)) &= \sqrt{S(x(t), z(t))} dt e^{jn(x(t), z(t))} \\
d\hat{B}(x(t), z(t)) &= \sqrt{S(x(t), z(t))} dt [\rho_N e^{jn(x(t), z(t))} \sqrt{1 - \rho_N^2} e^{j\psi(x(t), z(t))}] .
\end{aligned} \tag{25a}$$

Thus, the final representation of Equation (24) is given by

$$\begin{aligned}
A(x,z) &= \int_{-\infty}^{\infty} \sqrt{S(x(t), z(t))} dt e^{jn(x(t), z(t))} e^{jk_p x(t)} \\
B(x,z) &= \int_{-\infty}^{\infty} \rho_N \sqrt{S(x(t), z(t))} dt e^{jn(x(t), z(t))} e^{jk_p x(t)}
\end{aligned} \tag{25b}$$

and

$$\left. \int_{-\infty}^{\infty} \sqrt{1 - \rho_N^2} \sqrt{S(x(t), z(t))} dt e^{j\psi(x(t), z(t))} e^{jk_p x(t)} \right\}$$

where  $\rho_N$  is the cross-correlation between  $A$  and  $B$  (often zero),  $t$  is the variable of integration  $S(x(t), z(t))$  is the spectral density function (discussed below), and  $\varphi(x(t), z(t))$  and  $\psi(x(t), z(t))$  are uniformly random phase angles between 0 and  $2\pi$ . This derivation requires that the spectral density  $S(x(t), z(t))$  be an even function of  $t$ .

The material properties must be real (not imaginary) quantities. This causes some symmetry requirements in the equations, namely:

$$\begin{aligned}
\varphi(x(t), z(t)) &= \varphi[x(t), z(t)] \\
\psi(x(t), z(t)) &= \psi[x(t), z(t)] \\
S(\pm x(t), \pm z(t)) &= S[x(t), z(t)]
\end{aligned} \tag{26}$$

Using these equations, we can calculate a set of random material properties. The procedure is to find many random phase angles, (numerically) calculate the integrals in Equation (25b), and insert the result into Equation (24). We do these calculations at each position  $(x,z)$ . The integration variable  $(t)$  must sample and span the spectral density function sufficiently. This is discussed below in more detail.

### Wave field

To calculate the frequency response of the random medium over a uniformly sampled frequency range at a small number of specified positions, we express the vector wave displacement components as follows,

$$\begin{aligned} u_x(x, z, \omega) &= u_{0x}(x, z, \omega) [1 + U_x N(x, z, \omega)] \\ u_z(x, z, \omega) &= u_{0z}(x, z, \omega) [1 + U_z N(x, z, \omega)] \end{aligned} \quad (27)$$

where  $u_{0x}(x,z,\omega)$  and  $u_{0z}(x,z,\omega)$  are the deterministic responses, which may optionally contain the mean propagation phase, and  $U_x N(x,z,\omega)$  and  $U_z N(x,z,\omega)$  are the random field contributions, which were derived using a stochastic perturbation-theory solution of the wave equation.

The vector field components of the random field in terms of the density function and the random phases can be obtained directly using Equations (21a) and (22a). This requires only one integration in  $t$ . The rms amplitude of the random increments  $d\hat{A}(t)$  and  $d\hat{B}(t)$  are related directly to the spectral density function random field as addressed by Equation (25a). In these relationships,

$\theta(x(t), z(t))$  and  $\psi(x(t), z(t))$  are random phase angles of material properties A and B, which are distributed in  $[0, 2\pi]$  for any value of the functions  $x(t)$  and  $z(t)$ . These functions are given in Equations (B-9).

### Spectral density function

The spectral density function  $S(x(t), z(t))$  has a significant effect on the result. So far, we have used three classes of spectral density function: a Gaussian class, a Gauss-Markov class, and a spectral density function from Müller et al., 1992. The requirements of a spectral density function are that its integral over  $k$ -space must be one and its mean must be zero (an even function). All classes use fluctuation lengths  $L_x$  and  $L_z$  to characterize the medium.

The Gaussian form of spectral density function is given by

$$S(x(t), z(t)) = A k^{\alpha} e^{-\frac{\alpha}{2} k^2} \quad (28)$$

where  $k^2 = (x(t)L_x)^2 + (z(t)L_z)^2$  is a normalized magnitude in  $k$ -space. The parameter  $\alpha$  can take on a value of 0,  $\frac{1}{2}$ , 1, or 2. For each of these values, we have a different normalization constant  $A$ ,

as shown in Table 1. We have found that the  $\alpha=2$  case is probably the best choice. The Gauss-Markov form of spectral density function is given by

$$S(x(t), z(t)) = Ak^{\alpha} [1 + k^2]^{-\alpha/2} \quad (29)$$

The parameter  $\alpha$  can take on a value of 0,  $\frac{1}{2}$ , or 1. For each of these values, we have a different normalization constant  $A$ , as shown in Table 2.

Muller's (1992) spectral density function is given by

$$S(x(t), z(t)) = \frac{L_x L_z}{2\pi} \left\{ [1 + k^2]^{-3/2} \frac{\frac{3}{2}k^2 + 1}{[1 + k^2]^{7/2}} \right\} \quad (30)$$

Its major feature is that it decreases very slowly with increasing  $k$ .

### Choice of Modeling Input Parameters

The wave fields are obtained by integrating over by taking one-dimensional Fourier transforms. We approximate the transform using a complex one-dimensional FFT. This means we must ensure that the range of  $t$  is large enough so the integrand is zero beyond that point. Furthermore, we must ensure the resolution of  $t$ , namely  $\Delta t$ , is small enough to sample accurately the variations in the integrand. We consider the variation in the magnitude of the integrand to be largely due to the spectral density function. The resolution and range of  $t$  must be sufficient. Most of the important variation is in the spectral density function, several forms of which are illustrated. Because we are using an FFT, the resolution and range of  $t$  is tied directly to the spatial parameters and the fluctuation length.

## RESULTS

To test the numerical concepts, we construct a model by assuming that seismic energy is propagating between two vertical boreholes. For this purpose a plane-wave propagates in the  $x$ -direction perpendicular to the receiver borehole. The plane-wave propagates with a compressional wave velocity of 4000 m/s in a medium characterized by an S-wave velocity of 2000 m/s and a bulk density of  $2.65 \text{ g/cm}^3$ . Also, the medium is characterized by intrinsic quality factors  $Q_p = 100$  and  $Q_s = 50$ . To represent a random heterogenous medium we sample the half-space using a grid of 64 by 256 points at increments of 5 m. In addition, we use the correlation lengths of  $L_x = 20 \text{ m}$  and  $L_z = 10 \text{ m}$ , and a Gaussian spectral density function given by Equation 28. Since we are using the perturbation theory, we assume the standard deviations and the logarithm of the stiffness to be  $\sigma_A = \sigma_B = 0.1$ . The value of  $\sigma_A$  corresponds to the stiffness of  $\lambda + 2\mu$ , and  $\sigma_B$  corresponds to the rigidity  $\mu$ .

Figures 1a-c show three replicates of the random P-wave velocity. These are plots of the 2D random representation of the subsurface assuming a Gaussian distribution and the above correlation lengths. The random velocity images show heterogeneities that vary in the range of 3300 to 5225 m/s. This range is within  $3 \sigma_A$  of the random velocity distribution of the simulations.

This means that more than 99 percent of the random velocities are within plus or minus three standard deviations from the mean, and approximately 95 percent of all the heterogeneities are included in the interval lying within +2 to -2 standard deviations.

For a plane-wave propagating in the random heterogeneous medium, we simulate random displacement wave fields by applying a source pulse function having a center frequency of 75 Hz. The uncorrelated x-and z-component random fields are given in Figures 2a-c and 3a-c, respectively. The detector borehole is 200 m from the origin.

In general, the random wave field seismograms show several events associated with the structural distribution of heterogeneities, which can be explained by comparing the images given in Figures 1a-c with the corresponding random field seismograms. Since the correlation length in the horizontal direction is twice the correlation length in the vertical direction, the horizontal component seismogram is less affected by the presence of the small heterogeneities. On the other hand, the vertical component seismograms are more sensitive to the small statistical heterogeneities of the medium. This can be observed by wave dispersion or waveform broadening, which is simulated at different detector positions in the vertical random field component seismograms. The large scatterers observed in the 2D random velocity distribution produce strong reflections that can be better identified in the horizontal component seismograms.

To evaluate the simulations, tests are performed by comparing the synthetic seismogram for each replicate. For example, we expect that the amplitude of horizontal component waveforms will be greater than the amplitude of vertical component waveforms. By comparing Figures 2a and 3a, Figures 2b and 3b, and Figures 2c and 3c, it is observed that the amplitudes of the horizontal component seismograms are about two times greater than those of the vertical component seismograms. Although the direct events in both wave field components should arrive at the same time, in some traces it appears that the events of the horizontal random wave field arrive a bit earlier than those of the vertical random wave field. This occurs because the small scatterers associated with correlation lengths of  $L_z = 10$  m are captured by vertical component detectors, creating dispersive and attenuated seismic signatures. Thus, the first parts of the vertical component waveforms are more attenuated and the overall signatures are dispersive.

To further test the stochastic modeling approach, we compare the random velocity images with their corresponding seismic responses. In Figure 2a, the horizontal component seismogram shows a decrease in amplitude of the waveform at the receiver position of 180 m. Here it appears that there is a departure of two reflections, one event in the region from 0-180 m, and a second event in the region from 180-280 m. This signature is typical of a low-velocity zone in zero-vertical offset crosswell seismic profiles (see Parra et al., 1996). In fact, the corresponding velocity image of Figure 1a shows a light green zone of about 4125 m/s between 155m and 180 m, which is surrounded by several heterogeneities of dark green and blue colors in the range of 4400 m/s to 4950 m/s. The same signature is observed in the vertical component seismogram (Figure 3a), which correlates with the low-velocity zone in the region from 160-180 m in Figure 1a, and observed again at a detector depth of 420 m in Figure 2a. In Figure 1a, at 420 m, a velocity contrast is observed between the heterogeneities in blue/dark green and light green/yellow. Figures 1b and 1c compare similarly with the corresponding seismograms. Both sets of seismograms show signature characteristics of low-velocity zones. For example, Figure 2b shows a low-velocity zone signature that correlates with the light green zone at 160 m in Figure 2a. An interesting event that arrives early is observed between depths of 120 to 240 m in Figure 3b. The event is probably a group of head waves traveling at the velocity of the dark

green/blue heterogeneities. These events are also observed in Figure 3c, at detector depths of 160-220 m, where there is a large heterogeneity in the corresponding image in Figure 1c (replicate 3) that extends 150 m in the x direction.

Head waves are observed in the vertical component responses because the high-velocity elongated structure zones in which head waves propagate generate particle motion that can be captured by vertical detectors. The vertical detectors are more sensitive to horizontal boundaries than are the horizontal detectors, and as a result head waves traveling faster in the elongated high-velocity structure can be observed better in vertical component seismograms (see Parra, 1996). These types of signatures have been observed in zero-vertical offset seismograms at the Gypsy test site (Parra et al., 1996).

## CONCLUSIONS AND DISCUSSIONS

This paper successfully demonstrates that the random Fourier-Stieltjes representation is a practical approach to solving the inhomogeneous elastic wave equation. The theory demonstrates that it is possible to obtain exact solutions of the elastic wave equation in terms of random elastic properties of the medium distributed in the horizontal (x) and vertical (z) directions. New theoretical development is implemented by reducing the double integral Fourier-Stieltjes representation to a single integral. As a result, a tractable form of the solution is derived for numerical applications.

The results of this work demonstrate that the solution can be used to simulate 2D random heterogeneous media based on the standard deviations of the elastic properties and the density function. Also, this paper demonstrates that realistic random synthetic seismograms can be produced using the solution. The synthetic seismograms indicate a decrease in wave amplitude and wave dispersion caused by elastic scattering based on the representation of the statistical heterogeneous medium. The wave broadening effect is clearly observed in the vertical wave field component seismograms. The large scatterers produce strong reflections observed in the random horizontal wave field seismograms. Similar signatures have been observed in crosswell data recorded at the Gypsy test site in Oklahoma.

The 2D random property images (based on the standard deviation of the rock physical properties) span a large number of heterogeneities varying from a few centimeters to several meters (about four orders of magnitude). This precludes the direct use of finite difference (FD) techniques to calculate the seismic response of 2D random property images. However, 2D random property images can be converted to simple structures using the appropriated processing algorithm. Thus, the new structures can be handled by an FD code to give an approximate response of the random wavefield. Although a comparison of 2D random wavefield responses with the corresponding responses based on FD is an important step in verifying the 2D random wavefield solution, it requires substantial effort to implement an algorithm to produce the geometry to run the FD code, without losing the random characteristics of the model. We believe that development of this algorithm is a subject for a new paper, in which the algorithm is used not only to verify the 2D random wavefield solution but to study seismic responses based on 2D-random generated models with geological constraints (e.g., formation boundaries) as well. This can be a feasible approach as long as the FD code can handle small and large heterogeneities in the same model.

## ACKNOWLEDGMENTS

This study was supported by the Internal Research Program at Southwest Research Program in San Antonio Texas. The comments and suggestions of the reviewers of the Journal of Applied Geophysics are appreciated. Special thanks to J. Stefani for a constructive review of the paper.

## REFERENCES

- Aki, K., Richards, P.G., 1980. Quantitative Seismology. Vol .1, Freeman, New York.
- Brown, R.L., Seifert, D., 1997. Velocity dispersion: A tool for characterizing reservoir rocks. *Geophysics*, 62, 477-486.
- Hackert, C.L., Parra, J.O., 2000. Analysis of multiscale scattering and poroelastic attenuation in a real sedimentary rock sequence. *Journal of the Acoustical Society of America*, 107, 3028-3034.
- Hoffman, W.C., 1964. Wave propagation in a random continuous medium. In: Bellman, R. (Ed.), *Proceedings of Symposia in Applied Mathematics, Stochastic Processes in Math, Physics and Engineering*, Am. Math. Soc. , Providence, RI, Vol. 16, 1964, 117-144 .
- Ikelle, L.T., Yung, S.K, Dause, F., 1993. 2-D random media with ellipsoidal auto-correlation functions. *Geophysics*, 58, 1359-1372.
- Keller, J.R., 1964. Equations and wave propagation in random media. In: Bellman, R. (Ed.), *Proceedings of Symposia in Applied Mathematics, Stochastic Processes in Math, Physics and Engineering*, Am. Math. Soc., 145-170.
- Kerner, C., 1992. Anisotropy in sedimentary rocks modeled as random media. *Geophysics*, 58, 564-576.
- Kneib, G., Kerner, C., 1993. Accurate and efficient seismic modeling in random media. *Geophysics*, 58, 576-588.
- Korn, M., 1993. Seismic waves in random media. *Journal of Applied Geophysics*, 29, 247-269.
- Lerche, D.I., Petroy, D., 1986. Multiple scattering of seismic waves in fractured media: velocity and effective attenuations of coherent components of P-waves and S-waves. *PAGEOPH*, 124, 975-1018.
- Müller, G., Roth, M., Korn, M., 1992. Seismic-wave traveltimes in random media. *Geophysical Journal International*, 110, 22-41.
- O'Doherty, R.F., Anstey, N.A., 1971. Reflections on amplitudes. *Geophysical Prospecting*, 19, 430-458.
- Parra, J.O., 1996. Guided seismic waves in layered poroviscoelastic media for continuity logging applications: model studies. *Geophysical Prospecting*, 44, 403-425.
- Parra, J.O., Ababou, R., Sablik, M.J., Hackert, C.L., 1999a. A stochastic wave field solution of the acoustic wave equation based on the random Fourier-Stieltjes increments. *Journal of Applied Geophysics*, 42, 81-87.

- Parra, J.O., Hackert, C.L., Ababou, R., Sablik, M. J., 1999b. Dispersion and attenuation of acoustic waves in randomly heterogeneous media. *Journal of Applied Geophysics*, 42, 99-115.
- Parra, J.O., Zook, B.J., Collier, H.A., 1996. Interwell seismic logging for formation continuity at the Gypsy test site, Oklahoma. *Journal of Applied Geophysics*, 35, 45-52.
- Roth, M., Korn, M., 1993. Single scattering theory versus numerical modeling in 2-D random media. *Geophysics Journal International*, 112, 124-140.
- Santosa, F., Symes, W.W., 1991. A dispersive affective medium for wave propagation in periodic composites. *SIAM Journal of Applied Mathematics*, 51, 984-1005.
- Shinozuka, 1972. Digital simulation of random processes and its applications. *Journal of Sound and Vibrations*, 25, 111-128.
- Shapiro, S.A., Zien, H., Hubral, P., 1994, A generalized O' Doherty-Anstey formula for waves in finely layered media. *Geophysics*, 59, 1750-1762
- Shapiro, S.A., and Zien, H., 1993. The O' Doherty - Anstey formula and localization of seismic waves. *Geophysics*, 58, 736-740.

## APPENDIX A

### Fourier Space-Green's Function Solution and Spectral Representation of the Random Log-Coefficients

In this section we introduce the 2D random Fourier-Stieltjes representation defined by (see Parra, et al., 1999):

$$f(x, z) = \int_{-\infty}^{\infty} \int_{-\infty}^{\infty} e^{j(k_z z + k_x x)} \hat{df}(k_x, k_z, \omega), \quad (\text{A-1})$$

for a random medium having material properties in the  $x$  and  $z$  directions. The increments of displacement in terms of random increments  $\hat{df}(k_x, k_z)$  in the wave number domain  $(k_x, k_z)$  associated with each material property required to apply Fourier transform to the linear system of partial differential equations given by Equations (14) and (18). Thus, the transformation of these equations in the wave number domain  $k_x$  and  $k_z$  are given by

$$\langle \cdot \rangle \hat{du}_A = \hat{df}_A \quad (\text{A-2})$$

and

$$\langle \cdot \rangle \hat{du}_B = \hat{df}_B,$$

where

$$\hat{du}_A = [du_A^{(x)}, du_A^{(z)}]^T \quad (\text{A-2a})$$

$$\hat{du}_B = [du_B^{(x)}, du_B^{(z)}]^T \quad (\text{A-2b})$$

$$\hat{df}_A = [df_A^{(x)}, df_A^{(z)}]^T \quad (\text{A-2c})$$

and

$$\hat{df}_B = [df_B^{(x)}, df_B^{(z)}]^T. \quad (\text{A-2d})$$

The operator  $\langle \cdot \rangle^*$  in the wave number  $k_x, k_z$  is given by

$$\langle \cdot \rangle^* = \begin{pmatrix} \alpha_G k_x^2 + \mu_G k_z^2 + \omega^2 \rho_G & (\lambda_G + \mu_G) k_x k_z \\ (\lambda_G + \mu_G) k_x k_z & \alpha_G k_z^2 + \mu_G k_x^2 + \omega^2 \rho_G \end{pmatrix}. \quad (\text{A-3})$$

The solution of the linear system of equations given by Equation (A-2) can be expressed as

$$d\hat{u}_A = G(k_x, k_z) d\hat{f}_A$$

and

$$d\hat{u}_B = G(k_x, k_z) d\hat{f}_B, \quad (\text{A-4})$$

where the coefficients of the matrix  $G(k_x, k_z)$  are given by

$$g_{11} = \frac{\alpha_G k_z^2 + \mu_G k_x^2 + \omega^2 \rho_G}{\text{Det}(\cdot)} \quad (\text{A-5a})$$

$$g_{12} = \frac{(\lambda_G + \mu_G) k_x k_z}{\text{Det}(\cdot)}, \quad g_{21} \quad (\text{A-5b})$$

$$g_{22} = \frac{\alpha_G k_x^2 + \mu_G k_z^2 + \omega^2 \rho_G}{\text{Det}(\cdot)} \quad (\text{A-5c})$$

in which

$$\text{Det}(\cdot) = \alpha_G \mu_G (k_x^2 + k_z^2 + k_p^2) (k_x^2 + k_z^2 + k_s^2), \quad (\text{A-6})$$

and

$$k_p^2 = \frac{\omega^2 \rho_G}{\alpha_G}; \quad k_s^2 = \frac{\omega^2 \rho_G}{\mu_G}. \quad (\text{A-6a})$$

The next step in the theoretical analysis is to determine expressions for the Fourier-Stieltjes (FS) increments  $d\hat{f}_A(k_x, k_z)$ , and  $d\hat{f}_B(k_x, k_z)$ , in terms of the random material properties. For this, we define the following quantities:

C  $d\hat{A}(k_x, k_z)$ : the random F-S increment of zero-mean stationary field  $A(x, z)$ ;

C  $d\hat{B}(k_x, k_z)$ : the random Fourier-Stieltjes increment of the zero-mean stationary field  $B(x, z)$ .

Next, applying the theorem (Parra et al., 1999a)

$$d\hat{f}(\mathbb{R}) = u_0(\omega) d\hat{a}(k + k_0), \quad (\text{A-7})$$

where  $\hat{a}$  is a zero-mean Gaussian random field, the increments of  $d\hat{f}_A$  and  $d\hat{f}_B$  yields the following expressions:

$$\begin{aligned}
 d\hat{f}_A^{(x)} &= \alpha_G j k_x [u_o(\omega) k_o^2 d\hat{A}(k_x \% k_{ox}, k_z \% k_{oz})] \\
 d\hat{f}_A^{(z)} &= \alpha_G j k_z [u_o(\omega) k_o^2 d\hat{A}(k_x \% k_{ox}, k_z \% k_{oz})] \\
 d\hat{f}_B^{(x)} &= \mu_G j k_z [u_o(\omega) k_o^2 \sin 2\theta d\hat{B}(k_x \% k_{ox}, k_z \% k_{oz})] \\
 d\hat{f}_B^{(z)} &= \mu_G j k_x [u_o(\omega) k_o^2 \sin 2\theta d\hat{B}(k_x \% k_{ox}, k_z \% k_{oz})].
 \end{aligned}
 \tag{A-8}$$

## APPENDIX B

### First-Order Stochastic Vector Wave field

The random parts of the vector displacement components in terms of the coefficients of the Green's tensor are given by

$$\begin{pmatrix} d\hat{u}_x \\ d\hat{u}_z \end{pmatrix} = \begin{pmatrix} g_{11} & g_{12} \\ g_{21} & g_{22} \end{pmatrix} \begin{pmatrix} d\hat{s}_x \\ d\hat{s}_z \end{pmatrix}, \quad (\text{B-1})$$

where

$$d\hat{s}_x = \sigma_A d\hat{f}_A^{(x)} + \sigma_B d\hat{f}_B^{(x)} \quad (\text{B-2})$$

$$d\hat{s}_z = \sigma_A d\hat{f}_A^{(z)} + \sigma_B d\hat{f}_B^{(z)}.$$

The next step is to replace the increments  $d\hat{f}$  (given in Appendix A) into Equation (B-2) to yield the source terms as a function of the material property increments  $d\hat{A}$  and  $d\hat{B}$ :

$$\begin{aligned} d\hat{s}_x = & u_0(\omega) k_0^2 [ \alpha_G \sigma_A j k_x d\hat{A}(k_x, k_{ox}, k_z, k_{oz}) \\ & + \mu_G \sigma_B j k_z \sin 2\theta d\hat{B}(k_x, k_{ox}, k_z, k_{oz}) ] \end{aligned} \quad (\text{B-3a})$$

and

$$\begin{aligned} d\hat{s}_z = & u_0(\omega) k_0^2 [ \alpha_G \sigma_A j k_z d\hat{A}(k_x, k_{ox}, k_z, k_{oz}) \\ & + \mu_G \sigma_B j k_x \sin 2\theta d\hat{B}(k_x, k_{ox}, k_z, k_{oz}) ]. \end{aligned} \quad (\text{B-3b})$$

The displacement increments are given explicitly after we substitute the coefficients of the Greens' tensor and the source functions given in Equations (A-5), and (A-8) into Equation (B-1). The displacement random increments in the wavenumber domain gives the random wave fields using the inverse Fourier-Stieltjes representation:

$$u_x(x, z, \omega) = \int_{-\infty}^{\infty} \int_{-\infty}^{\infty} e^{j(k_x x + k_z z)} d\hat{u}_x(k_x, k_z, \omega), \quad (\text{B-4a})$$

where

$$\begin{aligned}
 d\hat{u}_x = u_o(\omega) \left\{ j\sigma_A \frac{k_p^2 k_x}{k_x^2 \% k_z^2 \% k_p^2} d\hat{A}(k_x \% k_{ox}, k_z \% k_{oz}) \right. \\
 \% j\sigma_B \sin 2\theta \left( \frac{v_s}{v_p} \right)^2 k_z \left( \frac{k_s^2 \% 2k_x^2}{k_x^2 \% k_z^2 \% k_s^2} \% \frac{2k_x^2}{k_x^2 \% k_z^2 \% k_p^2} \right) \\
 \left. \times d\hat{B}(k_x \% k_{ox}, k_z \% k_{oz}) \right\}
 \end{aligned} \tag{B-4b}$$

$$u_z(x, z, \omega) = \int_{\&4}^4 e^{j(k_x y \% k_z z)} du_z(k_x, k_z, \omega). \tag{B-5}$$

and

In Equation (B-4b)  $k_o$  has been replaced by  $k_p$ . The increment  $du_z(k_x, k_z, \omega)$  can be derived directly from the increment  $du_x(k_x, k_z, \omega)$  by substituting  $k_x \leftrightarrow k_z$ ,  $k_z \leftrightarrow k_x$ ,  $k_{ox} \leftrightarrow k_{oz}$ , and  $k_{oz} \leftrightarrow k_{ox}$  in Equation (B-4b).

The random wave field equations are expressed in terms of a stable Fourier-Stieltjes representation, which are reduced to single integrals by removing the singularities. This new representation for the integrals in Equations (B-4b) and (B-5), are given in Appendix A. Therefore, the final form of these integrals are used to construct the random wave field displacements  $u_x$  and  $u_z$  expressed in terms of single integrals that are appropriate for calculations. Thus, the random wave field are given by

$$\begin{aligned}
 u_x(x, z, \omega) = \int_{\&4}^4 \left\{ j\sigma_A k_p^2 d\hat{G}_1^{(x)}(t) \% j\sigma_B k_p^2 \sin 2\theta \left( \frac{v_s}{v_p} \right)^2 \right. \\
 \left. \times [d\hat{G}_2^{(x)}(t) \% d\hat{G}_3^{(x)}(t)] \right\} e^{jk_p x t},
 \end{aligned} \tag{B-6a}$$

where

$$d\hat{G}_1^{(x)}(t) = \frac{t\cos\theta + a\sin\theta}{\sqrt{t^2 + \left(1 + \frac{j}{2Q_p}\right)^2}} e^{&k_p|z|N\sqrt{t^2 + \left(1 + \frac{j}{2Q_p}\right)^2}} d\hat{A}(x_p(t), z_p(t)) \quad (\text{B-6b})$$

$$d\hat{G}_2^{(x)}(t) = \frac{(\&t\sin\theta + b\cos\theta) \left[ \frac{v_p^2}{v_s^2} + 2(t\cos\theta + b\sin\theta)^2 \right]}{\sqrt{t^2 + \frac{v_p^2}{v_s^2} \left(1 + \frac{j}{2Q_p}\right)^2}} \quad (\text{B-6c})$$

$$x e^{&k_p|z|N\sqrt{t^2 + \frac{v_p^2}{v_s^2} \left(1 + \frac{j}{2Q_s}\right)^2}} d\hat{B}(x_s(t), z_s(t))$$

$$d\hat{G}_3^{(x)}(t) = 2 \frac{(\&t\sin\theta + a\cos\theta)(t\cos\theta + a\sin\theta)^2}{\sqrt{t^2 + \left(1 + \frac{j}{2Q_p}\right)^2}} \quad (\text{B-6d})$$

$$x e^{&k_p|z|N\sqrt{t^2 + \left(1 + \frac{j}{2Q_p}\right)^2}} d\hat{B}(x_p(t), z_p(t))$$

in which

$$a = -\text{sign}(1-t^2) \sqrt{|1 + t^2|}$$

$$b = -\text{sign} \left( \frac{v_p^2}{v_s^2} + t^2 \right) \sqrt{\left| \frac{v_p^2}{v_s^2} + t^2 \right|} \quad (\text{B-6e})$$

$$x_p(t) = k_p [(1+a) \sin\theta + t \cos\theta]$$

$$z_p(t) = k_p [(1+a) \cos\theta - t \sin\theta]$$

$$x_s(t) = k_p \left[ \left( \frac{v_p}{v_s} + b \right) \sin\theta + t \cos\theta \right]$$

and

$$z_s(t) = k_p \left[ \left( \frac{v_p}{v_s} + b \right) \cos\theta - t \sin\theta \right].$$

In a similar manner we can express the random wave field for the vertical particle displacement  $u_z$ :

$$u_z(x, z, \omega) = \frac{\pi}{8} \left\{ j \sigma_A k_p^2 d \hat{G}_1^{(z)}(t) + j \sigma_B \sin 2\theta \left( \frac{v_s}{v_p} \right)^2 k_p^2 \right. \\ \left. \times [d \hat{G}_2^{(z)}(t) + d \hat{G}_3^{(z)}(t)] \right\} e^{jk_p x N}, \quad (\text{B-7a})$$

where  $xN = x \cos \theta - z \sin \theta$

$$zN = z \cos \theta + x \sin \theta,$$

and

$$d \hat{G}_1^{(z)} = \frac{t \sin \theta + a \cos \theta}{\sqrt{t^2 + \left( 1 + \frac{j}{2Qp} \right)^2}} e^{jk_p z N} \sqrt{t^2 + \left( 1 + \frac{j}{2Qp} \right)^2} d \hat{A}(x_p(t), z_p(t)) \quad (\text{B-7b})$$

$$d \hat{G}_2^{(z)} = \frac{(t \cos \theta + b \sin \theta) \left[ \frac{v_p^2}{v_s^2} + 2(t \sin \theta + b \cos \theta)^2 \right]}{\sqrt{t^2 + \frac{v_p^2}{v_s^2} \left( 1 + \frac{j}{2Qp} \right)^2}} \quad (\text{B-7c})$$

$$dG_3^{(z)}(z) = \frac{2(\cos\theta - j\sin\theta) (\sin\theta - j\cos\theta)^2 e^{k_p |z|N} \sqrt{t^2 \left(1 + \frac{j}{2Q_p}\right)^2}}{\sqrt{t^2 + \left(1 + \frac{j}{2Q_p}\right)^2}} d\hat{B}(x_p(t), z_p(t)) \quad (B-7d)$$

$$x e^{k_p |z|N} \sqrt{t^2 + \frac{v_p^2}{v_s^2} \left(1 + \frac{j}{2Q_p}\right)^2} d\hat{B}(x_s(t), z_s(t))$$

After inspecting Equations (B-6a)-(B-6d) and Equations (B-7a)-(B-7d), we reduce these equations further in a more practical form for computations. These equations in their new form are given by

$$\begin{aligned} d\hat{G}_1^{(x)}(t) &= G_1(t) d\hat{A}(x_p(t), z_p(t)) \\ d\hat{G}_1^{(z)}(t) &= G_1(t) d\hat{A}(x_p(t), z_p(t)) \\ d\hat{G}_2^{(x)}(t) &= G_2(t) d\hat{B}(x_s(t), z_s(t)) \\ d\hat{G}_2^{(z)}(t) &= G_2(t) d\hat{B}(x_s(t), z_s(t)) \\ d\hat{G}_3^{(x)}(t) &= G_3(t) d\hat{B}(x_p(t), z_p(t)) \\ d\hat{G}_3^{(z)}(t) &= G_3(t) d\hat{B}(x_p(t), z_p(t)), \end{aligned} \quad (B-8)$$

where the G functions are represented by

$$\begin{aligned} G_1(t) &= \frac{\cos\theta - j\sin\theta}{p} e^{k_p |z|N} \\ G_2(t) &= \frac{(\sin\theta - j\cos\theta)}{s} \left[ \frac{v_p^2}{v_s^2} + 2(\cos\theta - j\sin\theta)^2 \right] e^{k_p |z|N} \\ G_3(t) &= 2 \frac{(\sin\theta - j\cos\theta)}{p} (\cos\theta - j\sin\theta)^2 e^{k_p |z|N} \end{aligned} \quad (B-9)$$

in which

$$p = \sqrt{t^2 + \left(1 + \frac{j}{2Q_p}\right)^2}$$

$$\text{and } s = \sqrt{t^2 + \frac{v_p^2}{v_s^2} \left(1 + \frac{j}{2Q_p}\right)^2}.$$

Finally, we write the random wave field vector directly in terms of the  $d\hat{A}$  and  $d\hat{B}$  increments for numerical calculations

$$\begin{aligned}
 u_x(x, z, \omega) &= \pi j \sigma_A k_p^2 \int_{\&4}^4 G_1(t) d\hat{A}(x_p(t), z_p(t)) \\
 &+ \pi j \sigma_B k_p^2 \sin^2 \theta \left( \frac{v_s}{v_p} \right)^2 \int_{\&4}^4 [G_2(t) d\hat{B}(x_s(t), z_s(t)) \\
 &+ G_3(t) d\hat{B}(x_p(t), z_p(t))]
 \end{aligned} \tag{B-10}$$

$$\begin{aligned}
 u_z(x, z, \omega) &= \pi j \sigma_A k_p^2 \int_{\&4}^4 G_1(\&t) d\hat{A}(x_p(\&t), z_p(\&t)) \\
 &+ \pi j \sigma_B k_p^2 \sin^2 \theta \left( \frac{v_s}{v_p} \right)^2 \int_{\&4}^4 [G_2(\&t) d\hat{B}(x_s(\&t), z_s(\&t)) \\
 &+ G_3(\&t) d\hat{B}(x_p(\&t), z_p(\&t))]
 \end{aligned} \tag{B-11}$$

where

$$\begin{aligned}
 x_p(t) &= k_p [(1 - a) \sin \theta t \cos \theta] \\
 z_p(t) &= k_p [(1 - a) \cos \theta t \cos \theta] \\
 x_s(t) &= k_p \left[ \left( \frac{v_p}{v_s} a \right) \sin \theta t \cos \theta \right] \\
 z_s(t) &= k_p \left[ \left( \frac{v_p}{v_s} a \right) \cos \theta t \sin \theta \right].
 \end{aligned}$$

In order to generate wave field responses with the above integral solution we express the Fourier increments  $d\hat{A}$  and  $d\hat{B}$  in terms of the spectral density function (S) following the method of Shinozuka (1972).

## APPENDIX C

### Solution of Integrals I and J of the Random Wave Field

In order to develop the integrals given in Equations (B-4b) and (B-5), we express these equations in term of the integrals **I** and **J**. The integral **I** is formed by the first term of the integrand given by Equation (B-4b) and represents the contribution of the random material property A to the wave field. The integral **J** is formed by the second term of Equation (B-4b) and corresponds to the contribution of the random material property B to the wave field.

#### General form of I

$$I = \int \int \frac{k_x}{k_x^2 + k_z^2 + k_p^2} e^{j(k_x x + k_z z)} d\hat{A}(k_{ox} + k_x, k_{oz} + k_z) \quad (C-1)$$

where  $k_{ox} = k_p \sin \theta$  and  $k_{oz} = k_p \cos \theta$ . If we introduce the variables

$$k_x = k_N \cos \theta + k_N' \sin \theta \quad (C-2)$$

and  $k_z = k_N \cos \theta - k_N' \sin \theta$ ,

the integral I becomes

$$I = \int \int \frac{k_N \cos \theta + k_N' \sin \theta}{k_N^2 + k_N'^2 + k_p^2} e^{j(k_N x_N + k_N' z_N)} d\hat{A}[(k_p + k_N) \sin \theta + k_N' \cos \theta ; (k_p + k_N) \cos \theta + k_N' \sin \theta] , \quad (C-3)$$

where  $x_N = x \cos \theta - z \sin \theta$  (C-4)

$z_N = z \cos \theta + x \sin \theta$ .

In Equation (C-4),  $x_N$  is the distance of propagation in the direction transverse to the plane wave and  $z_N$  is the distance of propagation in the direction of the plane wave.

In Equation (C-3) two poles are observed. There is one pole in the first quadrant of the complex  $k_N$ -plane, given by

$$k_N = j\gamma + (k_p^2 + k_N'^2)^{1/2} . \quad (C-5)$$

and a second pole in the third quadrant of the  $k_N$ -plane is defined by

$$k_N = -j\gamma + (k_p^2 + k_x^2)^{1/2}$$

In both cases, we find that the  $\text{Re}(\gamma)$  is positive, and  $\text{Im}(\gamma)$  is negative. The integral (C-3) can be evaluated using the residue theorem. For  $z_N > 0$ , the factor  $\exp(jk_N z_N)$  suppresses the integrand in (C-3), if it is taken around a sufficiently large semicircle in the upper half-plane. Adding this semicircle to the integration path along the real axis, we have a closed path going in the positive direction around a pole at  $k_N = j\gamma$  in the first quadrant, such that

$$I_1 = 2\pi j \text{Residue} = \pi \int_{-\infty}^{\infty} \frac{k_N \cos\theta + j\gamma \sin\theta}{\gamma} e^{jk_N z_N} \times d\hat{A} \{ [(k_p + j\gamma) \sin\theta + k_x \cos\theta]; [(k_p + j\gamma) \cos\theta + k_x \sin\theta] \} \quad (\text{C-6})$$

; for  $z_N > 0$ .

The next pole is defined by  $k_N = -j\gamma$  and  $z_N < 0$ . Thus, we obtained a second integral

$$I_2 = -2\pi j \text{Residue} = \pi \int_{-\infty}^{\infty} \frac{k_N \cos\theta - j\gamma \sin\theta}{\gamma} e^{jk_N z_N} \times d\hat{A} \{ [(k_p - j\gamma) \sin\theta + k_x \cos\theta]; [(k_p - j\gamma) \cos\theta + k_x \sin\theta] \} . \quad (\text{C-7})$$

Summarizing these results, we construct a solution that can be appropriate to simulate random wave fields. This requires to have a solution that must converge for large  $z_N$  so we choose the

exponent to be  $\exp(-\gamma |z_N|)$ . Since  $j\gamma = \sqrt{k_p^2 + k_x^2}$ , and the function  $d\hat{A} [(k_p + \sqrt{k_p^2 + k_x^2}) \sin\theta + k_x \cos\theta; (k_p + \sqrt{k_p^2 + k_x^2}) \cos\theta + k_x \sin\theta]$  is equal  $d\hat{A}(0,0)$  for  $k_N = 0$ , and the same function is finite and analytical for  $k_N = \pm k_p$ , the integrals  $I_1$  and  $I_2$  can be

used to calculate the integral  $I$  in the range  $(-4, 4)$ . The final integral can be written as

$$I = \pi \int_{-\infty}^{\infty} d\hat{G}(k_N, k_p, \theta) e^{jk_N x_N} e^{\sqrt{k_N^2 + \tilde{k}_p^2} z_N} \quad (C-8)$$

where

$$d\hat{G} = \begin{cases} \frac{k_N \cos\theta + \sqrt{k_p^2 + k_N^2} \sin\theta}{\sqrt{k_N^2 + \tilde{k}_p^2}} d\hat{A}[(k_p + \sqrt{k_p^2 + k_N^2}) \sin\theta + k_N \cos\theta; \\ (k_p + \sqrt{k_p^2 + k_N^2}) \cos\theta + k_N \sin\theta]; \\ \text{for } k_N \neq |k_p| \\ \frac{k_N \cos\theta - \sqrt{k_N^2 + k_p^2} \sin\theta}{\sqrt{k_N^2 + \tilde{k}_p^2}} d\hat{A}[(k_p + \sqrt{k_p^2 + k_N^2}) \sin\theta + k_N \cos\theta; \\ (k_p + \sqrt{k_p^2 + k_N^2}) \cos\theta + k_N \sin\theta]; \\ \text{for } k_N \leq |k_p| \end{cases}$$

in which  $\tilde{k}_p = (1 + \frac{j}{2Q_p})$ .

The next step is to replace  $k_N = k_p t$

$$I = \pi \int_{-\infty}^{\infty} dG(t) e^{j(k_p x_N) t} \quad (C-9)$$

where

$$dG(t) = \frac{t \sin \theta + a \sin \theta}{\sqrt{t^2 + (1 + \frac{j}{2Qp})^2}} e^{jk_p |z| \sqrt{t^2 + (1 + \frac{j}{2Qp})^2}} d\hat{A}(x(t), z(t)), \quad (C-10)$$

in which

$$\begin{aligned} a &= \text{sign}(1 + t^2) \sqrt{|1 + t^2|} \\ x(t) &= k_p [(1 + a) \sin \theta + t \cos \theta] \\ z(t) &= k_p [(1 + a) \cos \theta + t \sin \theta] \end{aligned} \quad (C-11)$$

and  $k_p = \frac{\omega}{v_p}$ .

The rms amplitude of the random Fourier increment  $d\hat{A}(t)$  represents the spectral content of fluctuations of  $I(x|N)$  in the range  $(t, t + dt)$ .

### General form of J

$$J = \int_{-4}^4 k_z \left( \frac{k_s^2 + 2k_x^2}{k_x^2 + k_z^2 + k_s^2} + \frac{2k_x^2}{k_x^2 + k_z^2 + k_p^2} \right) e^{j(k_x x + k_z z)} d\hat{B}(\vec{k} + \vec{k}_0) \quad (C-12)$$

where  $d\hat{B}(\vec{k} + \vec{k}_0) / d\hat{B}(k_{ox} + k_x; k_{oz} + k_z)$

and  $k_{ox} = k_p \sin \theta$  and  $k_{oz} = k_p \cos \theta$ .

This integral is formed by two integrals

$$J_1 = \int_{-4}^4 \frac{k_z (k_s^2 + 2k_x^2)}{k_x^2 + k_z^2 + k_s^2} e^{j(k_x x + k_z z)} d\hat{B}(\vec{k} + \vec{k}_0) \quad (C-13)$$

and

$$J_2 = \int_{-4}^4 \frac{2k_z k_x^2}{k_x^2 + k_z^2 + k_p^2} e^{j(k_x x + k_z z)} d\hat{B}(\vec{k} + \vec{k}_0). \quad (C-14)$$

The integrals  $J_1$  and  $J_2$  can be converted to single integrals by following the same procedure as that applied to obtain integral I. We first make the transformation that expresses the integrals in terms of the angle of incidence  $\theta$ , then we transform the integrals in terms of the parameter  $t$ . This will be the final stage of integrals to determine the vector wave field. Following this procedure the integrals are given first by

$$J_1 = \pi \int_{-\pi/4}^{\pi/4} dG_1(k_N, k_p, \theta) e^{jk_N x N e^{\frac{|z|N\sqrt{k_N^2 + \tilde{k}_p^2}}{\sqrt{k_N^2 + \tilde{k}_s^2}}} \quad (C-15)$$

$$dG_1 / \left\{ \begin{array}{l} (\& k_N \sin\theta + \sqrt{k_s^2 + k_N^2} \cos\theta) (k_s^2 + 2 (k_N \cos\theta + \sqrt{k_s^2 + k_N^2} \sin\theta)^2) \\ \quad \times d\hat{B} \left\{ (k_s + \sqrt{k_s^2 + k_N^2}) \sin\theta - k_N \cos\theta ; \right. \\ \quad \left. (k_s + \sqrt{k_s^2 + k_N^2}) \cos\theta + k_N \sin\theta \right\} ; \text{ for } k_N \neq |k_s| \\ (\& k_N \sin\theta - \sqrt{k_s^2 + k_N^2} \cos\theta) (k_s^2 + 2 (k_N \cos\theta + \sqrt{k_s^2 + k_N^2} \sin\theta)^2) \\ \quad \times d\hat{B} \left\{ (k_s - \sqrt{k_s^2 + k_N^2}) \sin\theta - k_N \cos\theta ; \right. \\ \quad \left. (\& k_N \sin\theta - \sqrt{k_s^2 + k_N^2} \cos\theta) + k_N \sin\theta \right\} ; \text{ for } k_N \neq |k_s| \end{array} \right.$$

and

$$J_2 = \pi \int_{-\pi/4}^{\pi/4} dG_2(k_N, k_p, \theta) e^{-jk_N x N e^{\frac{|z|N\sqrt{k_N^2 + \tilde{k}_p^2}}{\sqrt{k_N^2 + \tilde{k}_s^2}}} \quad (C-16)$$

where

$$dG_2 / \left\{ \begin{array}{l} 2 (k_x \sin\theta + \sqrt{k_s^2 - k_x^2} \cos\theta) (k_s^2 + 2 (k_x \cos\theta + \sqrt{k_s^2 - k_x^2} \sin\theta)^2) \\ \quad \times d\hat{B} \{ (k_s + \sqrt{k_s^2 - k_x^2}) \sin\theta - k_x \cos\theta ; \\ \quad (k_s + \sqrt{k_s^2 - k_x^2}) \cos\theta + k_x \sin\theta \} ; \text{ for } k_x \neq |k_s| \\ \\ 2 (k_x \sin\theta - \sqrt{k_s^2 - k_x^2} \cos\theta) (k_s^2 + 2 (k_x \cos\theta + \sqrt{k_s^2 - k_x^2} \sin\theta)^2) \\ \quad \times d\hat{B} \{ (k_s - \sqrt{k_s^2 - k_x^2}) \sin\theta - k_x \cos\theta ; \\ \quad (k_x \sin\theta - \sqrt{k_s^2 - k_x^2} \cos\theta) + k_x \sin\theta \} ; \text{ for } k_x \neq |k_s| \end{array} \right.$$

Once the integrals  $J_1$  and  $J_2$  are constructed in terms of the angle of incidence  $\theta$ , they can be expressed in a more compact form as integral I, given by Equations (C-10) and (C-12). These integrals written in a compact form are given by, for  $J_1$ :

$$J_1 = \pi \int_0^{\pi/4} dG_1(t) e^{jk_p x(t)} \quad (C-17)$$

where

$$dG_1(t) = k_p^2 \frac{(\sin\theta - b \cos\theta) \left[ \frac{v_p^2}{v_s^2} (t \cos\theta - b \sin\theta)^2 \right]}{\sqrt{t^2 + \frac{v_p^2}{v_s^2} \left(1 + \frac{j}{2Q_s}\right)^2}} e^{-k_p |z(t)| \sqrt{t^2 + \frac{v_p^2}{v_s^2} \left(1 + \frac{j}{2Q_s}\right)^2}} \times d\hat{B}(x(t), z(t))$$

in which

$$x(t) = k_p \left[ \left( \frac{v_p}{v_s} + b \right) \sin\theta + t \cos\theta \right]$$

$$z(t) = k_p \left[ \left( \frac{v_p}{v_s} + b \right) \cos\theta + t \sin\theta \right]$$

where

$$b = \text{sign} \left( \frac{v_p^2}{v_s^2} + t^2 \right) \sqrt{\left| \frac{v_p^2}{v_s^2} + t^2 \right|}$$

The next integral J is given by

$$J_2 = \pi \int_{-\infty}^{\infty} dG_2(t) e^{jk_p x(t)}$$

where

$$dG_2(t) = 2 \frac{(\sin\theta + a \cos\theta)(t \cos\theta + a \sin\theta)^2 k_p^2 e^{-k_p |z(t)| \sqrt{t^2 + (1 + \frac{j}{2Q_p})^2}}}{\sqrt{t^2 + (1 + \frac{j}{2Q_p})^2}}$$

$$x = \hat{B}(x(t), z(t)),$$

in which

$$a = \text{sign}(2 + t^2) \sqrt{|1 + t^2|}$$

$$x(t) = k_p [(1 + a) \sin\theta + t \cos\theta]$$

and

$$z(t) = k_p [(1 + a) \cos\theta + t \sin\theta].$$

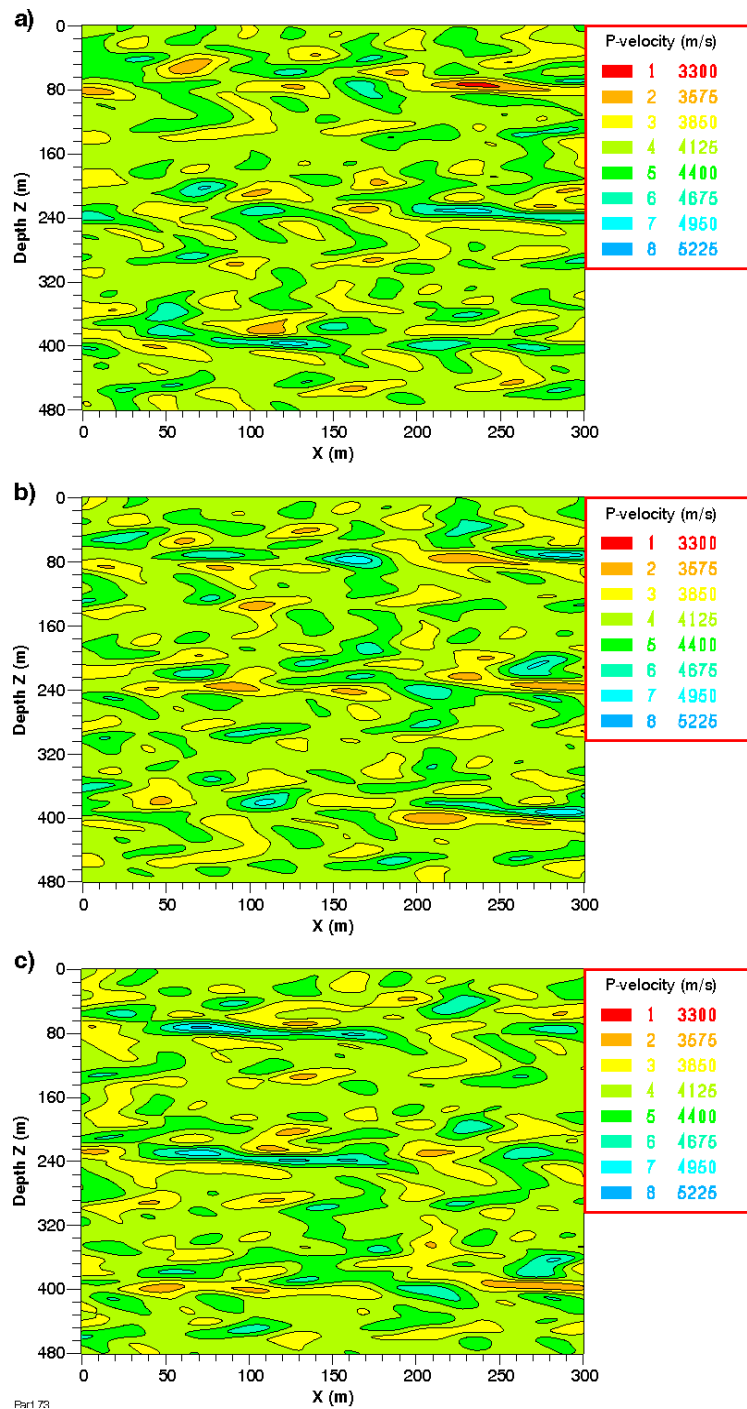
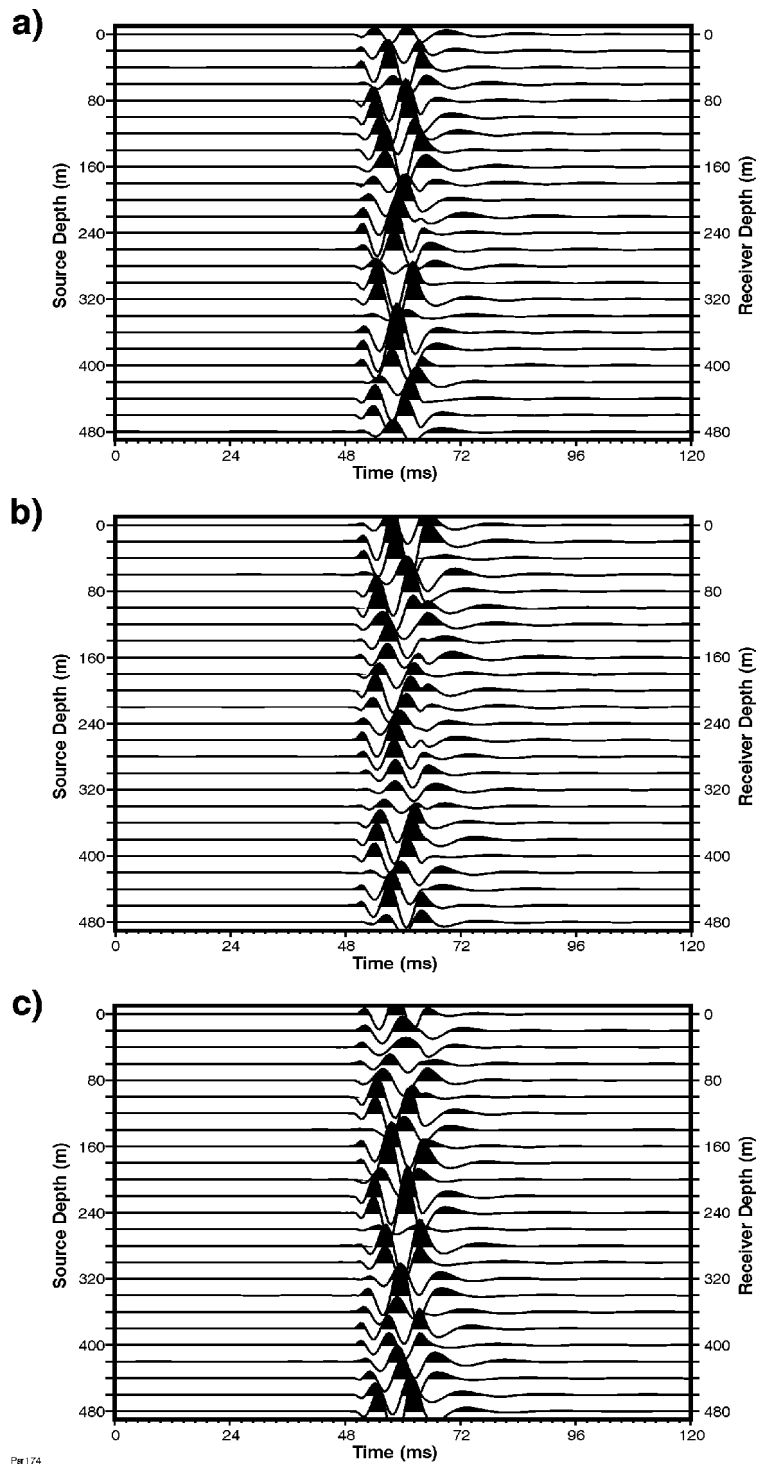
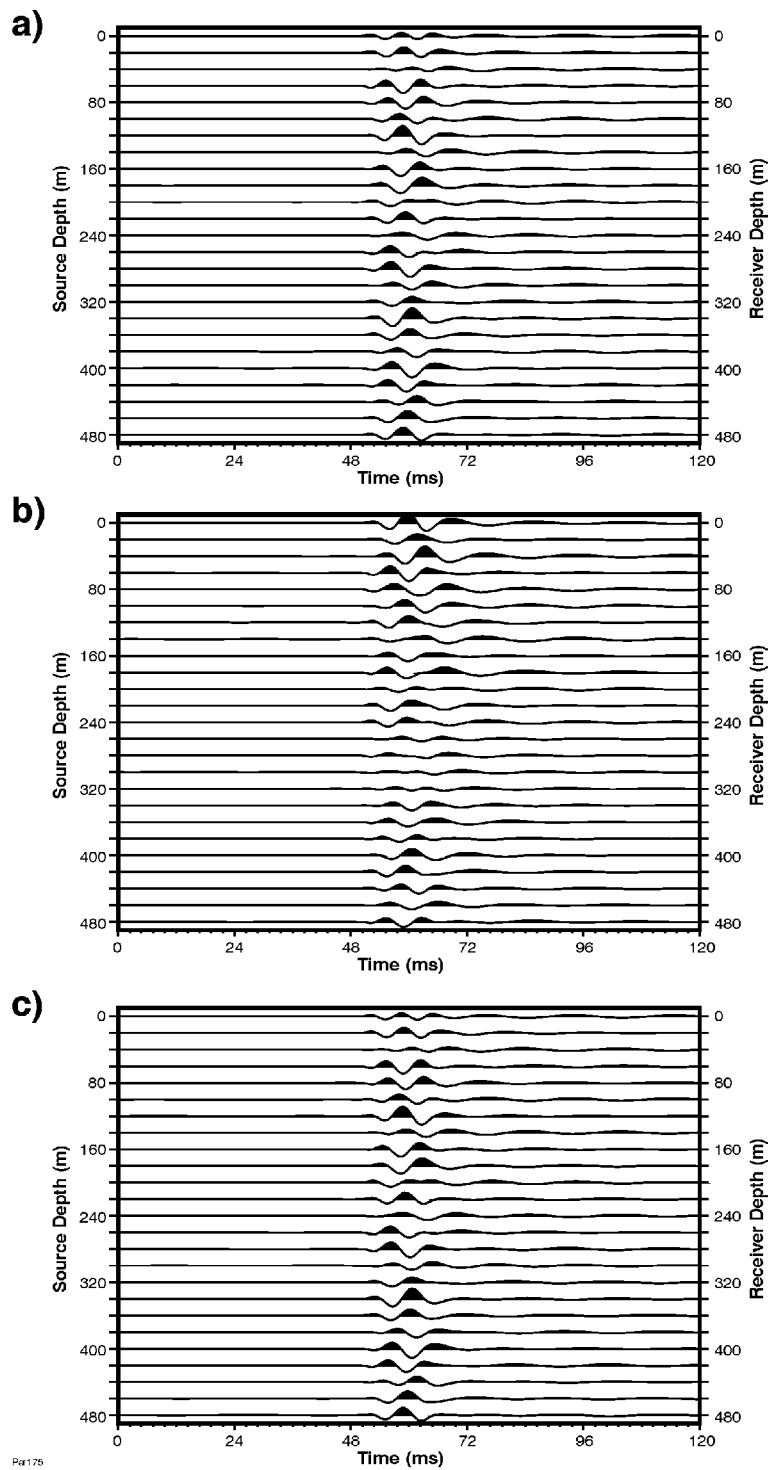


Figure 1. A 2D imaging of the random P-wave velocity distribution between two boreholes represented by a random medium for a) Replicate 1, b) Replicate 2, and c) Replicate 3.



Par174

Figure 2. The random vertical wave field component seismogram based on a source function having a center frequency of 75 Hz for a) Replicate 1, b) Replicate 2 , and 3) Replicate 3.



Par176

Figure 3. The random horizontal wave field component seismogram based on a source function having a center frequency of 75 Hz for a) Replicate 1, b) Replicate 2 , and 3) Replicate 3.

<b>Table 1: Normalization Constant for Gaussian Spectral Density</b>	
$\alpha$	A
0	$\frac{L_x L_z}{2\pi}$
$\frac{1}{2}$	$\frac{L_x L_z}{2\pi} \frac{1}{2^{1/4} (1/4)!} \cdot 0.14765 L_x L_z$
1	$\frac{L_x L_z}{2\pi} \sqrt{\frac{2}{\pi}}$
2	$\frac{L_x L_z}{4\pi}$

<b>Table 2: Normalization Constant for Gauss-Markov Spectral Density</b>	
$\alpha$	A
0	$2 \frac{L_x L_z}{2\pi}$
$\frac{1}{2}$	$\frac{8}{\pi\sqrt{2}} \frac{L_x L_z}{2\pi}$
1	$\frac{4}{\pi} \frac{L_x L_z}{2\pi}$